Journal of Experimental and Computational Methods in Applied Sciences, pp. 1–15

Modeling and Interpretation of Transient Near-Wellbore Phenomena for Improved Well Control and Formation Evaluation

Rafael Sousa [1], Diego Mendes [2]

1. *Universidade Federal do Pampa (UNIPAMPA), 275 Avenida Antônio Trilha, Centro, São Gabriel 97300-000, Brazil*
2. *Instituto Federal do Espírito Santo (IFES), 1200 Avenida Vitória, Jucutuquara, Vitória 29040-780, Brazil*

Abstract

Transient near-wellbore phenomena strongly influence measured pressures, temperatures, and flow rates in wells during drilling, completion, and production operations. These short-time responses encode information about local formation properties, near-wellbore damage or stimulation, and dynamic interactions between the wellbore and the surrounding porous medium. At the same time, they govern early-time well control behaviour, including detection of influxes, losses, and unstable flow regimes. Modeling and interpretation of these phenomena require rigorous treatment of multiphase flow, thermal and mechanical coupling, and the finite dimensions and storage of the wellbore. This work develops a mathematical and computational framework for describing transient near-wellbore processes and provides strategies for extracting formation and operational parameters from high-frequency measurements. The framework combines partial differential equation models for porous media flow and energy transport with reduced-order descriptions of the wellbore and its control logic. Numerical schemes tailored to the strong gradients and short time scales near the wellbore are discussed alongside data-driven surrogates that approximate the full physics. The analysis explores how different sources of non-ideal behaviour, such as skin, partial penetration, non-Darcy effects, and geomechanical coupling, distort the early-time signatures used in conventional interpretation. Machine-learning-based inversion and statistical analysis are used to map transient responses to uncertain formation properties in a probabilistic manner. The resulting methodology is intended to inform well control strategies and formation evaluation workflows that explicitly account for near-wellbore transients, without overstating their predictive capability, and to clarify the limits of interpretability under realistic levels of noise, operational constraints, and model uncertainty.

Introduction

Near-wellbore regions of subsurface formations play a disproportionate role in determining well performance, well control response, and the quality of formation evaluation [1]. Even when the reservoir far from the well is relatively homogeneous, the small volume around the wellbore can exhibit altered permeability, damaged or stimulated rock, complex saturation histories, and temperature perturbations induced by drilling and completion operations. Measurements acquired at the wellhead or downhole, such as pressure, flow rate, and temperature, are shaped by the transient flow and transport processes occurring over radial distances that may be only a few borehole radii. The short time scales associated with these processes give rise to characteristic signatures that are sensitive to local properties and boundary conditions, but their interpretation is challenging due to the superposition of multiple physical mechanisms and operational effects.

Classical well test analysis has established a rich set of analytical and semi-analytical solutions for transient flow to a well in infinite or bounded reservoirs, focusing primarily on late-time behaviour where the flow appears radial, linear, or spherical at a scale much larger than the wellbore. These solutions underpin many of the traditional approaches for estimating permeability, skin, and boundary distances [2]. However, they often idealize the near-wellbore region through simplified skin factors and wellbore storage coefficients, and they typically assume single-phase, isothermal, and linear Darcy flow. In early-time and high-frequency regimes, especially in modern wells with complex completion architectures, these assumptions are limited. Deviations from ideal behaviour appear in the recorded signals as non-classical slope changes, rate-dependent hysteresis, or coupled pressure and temperature

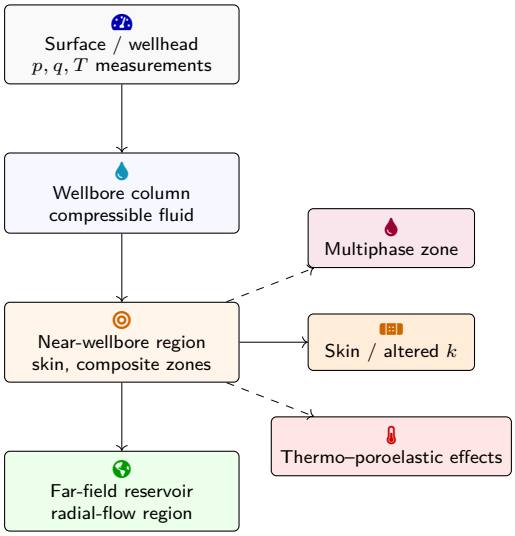

Figure 1: Conceptual structure of the near-wellbore system showing surface measurements, the wellbore fluid column, the altered near-wellbore zone with skin and multiphase or thermo–poroelastic effects, and the transition to the far-field reservoir where classical radial-flow assumptions typically apply.

Table 1: Key quantities in single-phase radial near-wellbore flow

Symbol	Description	Units
ϕ	Porosity	$-$
k	Permeability	m^2
c_t	Total compressibility	Pa^{-1}
μ	Viscosity	$\mathrm{Pa\,s}$
$p(r,t)$	Formation pressure	Pa
$q_s(r,t)$	Volumetric source/sink term	$\mathrm{m}^3\,\mathrm{s}^{-1}\,\mathrm{m}^{-3}$

transients that are not captured by traditional models.

The development of advanced instrumentation and downhole telemetry has increased the availability of high-resolution transient data near the wellbore. Distributed temperature and acoustic measurements, multipoint downhole pressure sensors, and fast surface measurement systems can resolve pressure and temperature dynamics over time scales down to seconds or less. In principle, such data enable more detailed characterization of formation properties and early detection of unwanted events such as influxes or losses [3]. In practice, extracting this information requires models that resolve the relevant physics at appropriate scales while remaining computationally tractable for online or near-real-time use. This balance motivates the use of hierarchical modeling strategies that combine detailed numerical solutions with reduced-order and data-driven representations.

The present work considers a set of coupled governing equations for flow and energy transport in the near-wellbore region, coupled to reduced-dimensional wellbore models that represent the dynamics of fluid columns and boundary conditions imposed by well control equipment. The formulation is based on conservation of mass and energy in a porous medium, combined with constitutive relations for Darcy or non-Darcy flow, phase behaviour, and, when relevant, poroelastic effects that couple pressure and mechanical deformation. These equations are specialized to configurations of practical interest, such as radial flow in cylindrical coordinates with wellbore storage and skin, partially penetrating completions, or composite near-wellbore regions with altered permeability and porosity.

Beyond deterministic modeling, the work addresses the interpretation of transient data through both analytical and data-driven approaches [4]. Analytical solutions and asymptotic analyses are used to clarify the influence of individual physical mechanisms and to derive dimensionless groups that capture key behaviours. Numerical simulations provide synthetic data sets for training and evaluating machine-learning models that map measured transients to underlying formation and operational parameters. Statistical frameworks are introduced to quantify uncertainty in such inversions and to assess identifiability limits given realistic measurement noise and model errors. The overall objective is to provide a coherent basis for integrating transient near-wellbore modeling into well control and formation evaluation workflows, emphasizing both capabilities and limitations.

Table 2: Wellbore coupling and storage parameters

Symbol	Description	Expression	Units
r_w	Wellbore radius	given	m
h	Effective producing height	given	m
C_w	Wellbore storage coefficient	modelled	$\mathrm{m}^3\,\mathrm{Pa}^{-1}$
$p_w(t)$	Sandface pressure	ODE variable	Pa
$q_r(t)$	Inflow from formation	$-2\pi r_w h \frac{k}{\mu}\frac{\partial p}{\partial r}\big\vert_{r_w}$	$\mathrm{m}^3\,\mathrm{s}^{-1}$
$q_{s,\mathrm{surf}}(t)$	Surface-controlled rate	control input	$\mathrm{m}^3\,\mathrm{s}^{-1}$

Table 3: Composite near-wellbore region and skin representation

Region	Parameter	Meaning	Typical relation
Inner ($r_w \le r \le r_s$)	k_s	Skin-zone permeability	$k_s k_r$
Inner	ϕ_s	Skin-zone porosity	modified vs. ϕ_r
Inner	$c_{t,s}$	Skin-zone compressibility	altered storage
Outer ($r \ge r_s$)	k_r	Far-field permeability	reference value
Outer	ϕ_r	Far-field porosity	reference value
Interface $r = r_s$	$p_s = p_r$	Pressure continuity	boundary condition
Interface $r = r_s$	$k_s \partial_r p_s = k_r \partial_r p_r$	Flux continuity	boundary condition

Physical processes and mathematical formulation of near-wellbore flow

A typical starting point for modeling transient near-wellbore flow in a slightly compressible single-phase system is the combination of mass conservation and Darcy's law in a cylindrical coordinate system centered on the well. For a porous medium with porosity ϕ, permeability k, and total compressibility c_t, the pressure field $p(r,t)$ in radial coordinate r and time t satisfies a diffusion-type equation derived from conservation of mass. Assuming negligible gravity within the near-wellbore zone and constant viscosity μ, the radial mass conservation equation can be written as [5]

$$\phi c_t \frac{\partial p}{\partial t} = \frac{1}{r}\frac{\partial}{\partial r}\left(r\frac{k}{\mu}\frac{\partial p}{\partial r}\right) + q_s(r,t), \tag{1}$$

where $q_s(r,t)$ represents distributed source or sink terms associated with wells or interfacial exchange between regions. The radial dependence in the operator captures the geometric spreading of flow away from the wellbore, and the combination ϕc_t defines a storage capacity per unit volume.

The presence of a finite wellbore radius r_w and wellbore storage leads to coupling between the porous medium and the fluid column inside the well. If $p_w(t)$ denotes the pressure at the sandface, the mass balance in the wellbore under a compressible or partially compressible fluid model can be approximated by an ordinary differential equation of the form

$$C_w \frac{dp_w}{dt} = q_r(t) - q_{s,\,surf}(t), \tag{2}$$

where C_w is an effective wellbore storage coefficient, $q_r(t)$ denotes the radial inflow from the formation into the wellbore at the sandface, and $q_{s,\,surf}(t)$ is the surface-controlled flow rate imposed by well control equipment. The radial inflow is related to the pressure gradient at the wellbore boundary by

$$q_r(t) = -2\pi r_w h \frac{k}{\mu}\frac{\partial p}{\partial r}\bigg|_{r=r_w}, \tag{3}$$

with h the effective producing height [6]. This boundary condition closes the coupling between the partial differential equation in the formation and the ordinary differential equation in the wellbore.

Near-wellbore deviations from ideal radial flow are often represented by a skin region of thickness δ around the wellbore where properties differ from those of the far-field reservoir. In a simple composite model, the permeability in this region, k_s, may be smaller or larger than the far-field permeability k_r, while porosity and compressibility can also be modified. Let $r_s = r_w + \delta$ denote the outer radius of the altered zone. The governing equation is then defined piecewise for $r_w \le r \le r_s$ and $r \ge r_s$ with properties $(k_s, \phi_s, c_{t,s})$ and $(k_r, \phi_r, c_{t,r})$, respectively. Continuity of pressure and radial flux at $r = r_s$ imposes interface conditions

$$p_s(r_s^-, t) = p_r(r_s^+, t), \tag{4}$$

$$k_s \frac{\partial p_s}{\partial r}\bigg|_{r=r_s^-} = k_r \frac{\partial p_r}{\partial r}\bigg|_{r=r_s^+}. \tag{5}$$

These relations define a local perturbation that modifies the effective pressure drop near the wellbore and gives rise to skin behaviour observable in transient tests.

Thermal effects add another layer of complexity to near-wellbore dynamics [7]. When injected or produced fluids have temperatures that differ from the initial formation temperature, energy transport in the porous medium and

Table 4: Thermal and thermo-hydro-mechanical quantities

Symbol	Description	Role	Units
$T(r,t)$	Temperature field	State variable	K
ρC_p	Effective volumetric heat capacity	Storage in energy balance	$\mathrm{J\,m^{-3}\,K^{-1}}$
λ_{eff}	Effective thermal conductivity	Conduction term	$\mathrm{W\,m^{-1}\,K^{-1}}$
$\mathbf{v}$	Darcy velocity	Advection of heat	$\mathrm{m\,s^{-1}}$
$q_T(r,t)$	Heat source/sink	Thermal forcing	$\mathrm{W\,m^{-3}}$
ϵ_v	Volumetric strain	Poroelastic coupling	–
α	Biot-type coefficient	Pressure–strain link	–

Table 5: Dimensionless variables and key groups for radial flow

Quantity	Definition	Interpretation
r_D	r/r_w	Dimensionless radius
t_D	$\dfrac{kt}{\phi\mu c_t r_w^2}$	Diffusion-scaled time
p_D	$(p-p_i)/\Delta p_{\text{ref}}$	Scaled pressure drop
C_D	$C_w/(2\pi\phi c_t r_w^2 h)$	Dimensionless storage
S	Skin factor (log-composite)	Near-wellbore resistance
Fo_T	$\lambda_{\text{eff}} t/(\rho C_p r_w^2)$	Thermal Fourier number

wellbore can alter fluid properties and induce thermoelastic stresses. An energy balance written for the porous medium, assuming local thermal equilibrium between fluid and solid and effective volumetric heat capacity ρC_p, leads to

$$\rho C_p \frac{\partial T}{\partial t} = \nabla \cdot (\lambda_{\text{eff}} \nabla T) - \rho C_p\, \mathbf{v} \cdot \nabla T[8] + q_T(r,t), \quad (6)$$

where $T(r,t)$ is temperature, λ_{eff} is an effective thermal conductivity, $\mathbf{v}$ is the Darcy velocity, and q_T represents heat sources or sinks. In near-wellbore regions, the advective term associated with radial flow can be important, and the interplay between pressure-driven flow and temperature evolution can produce characteristic transient signatures. The Joule–Thomson effect and fluid property variations with temperature and pressure can be included through appropriate dependence of μ and ρ on p and T, though in many near-wellbore applications a linearization is sufficient for analytical studies.

In many formations, mechanical deformation induced by pressure changes can significantly influence porosity and permeability. Poroelasticity provides a framework for capturing such coupling. A simple linear relationship between volumetric strain ϵ_v and fluid pressure, for a fixed stress state, can be written as

$$\epsilon_v = \alpha \frac{p - p_0}{M}, \quad (7)$$

where α is a Biot-type coefficient, M is a modulus characterizing the compressibility of the porous skeleton, and p_0 is a reference pressure. The porosity and permeability may then be expressed as functions of ϵ_v, such as

$$\phi(p)[9] = \phi_0 + c_\phi (p - p_0), \quad (8)$$

$$k(p) = k_0 \exp\left(c_k (p - p_0)\right), \quad (9)$$

with ϕ_0 and k_0 the reference porosity and permeability and c_ϕ and c_k small coefficients. Substituting these relations into the flow equation converts it into a nonlinear diffusion equation, in which the diffusivity depends on pressure. This nonlinearity can modify the shape of early-time transients and introduce asymmetry between drawdown and buildup responses.

For multiphase near-wellbore flow, the governing equations involve separate conservation laws for each phase, coupled through saturation constraints and relative permeability and capillary pressure relationships [10]. If S_α denotes the saturation of phase α, ρ_α its density, and $\mathbf{v}_\alpha$ its Darcy velocity, the mass balance of phase α takes the form

$$\phi \frac{\partial}{\partial t} (\rho_\alpha S_\alpha) + \nabla \cdot (\rho_\alpha \mathbf{v}_\alpha) = q_\alpha, \quad (10)$$

with q_α a source term. The Darcy velocity is given by [11]

$$\mathbf{v}_\alpha = -\frac{k k_{r\alpha}}{\mu_\alpha} \left(\nabla p_\alpha - \rho_\alpha \mathbf{g}\right), \quad (11)$$

where $k_{r\alpha}(S_\alpha)$ is the relative permeability and p_α is the phase pressure. In the immediate vicinity of the well, capillary pressures, relative permeability hysteresis, and dynamic saturation effects can lead to strong coupling between pressure and saturation transients, which in turn influence measured wellbore signals.

Dimensionless variables facilitate analysis of near-wellbore phenomena by separating geometric and property effects from operational conditions. A common choice introduces a dimensionless radius $r_D = r/r_w$, a dimensionless time t_D proportional to $kt/(\phi\mu c_t r_w^2)$, and a dimensionless pressure scaled by a characteristic pressure drop. The diffusion equation then takes a normalized form such

Table 6: Numerical discretization features for near-wellbore simulations

Aspect	Options	Comment	Typical choice
Spatial scheme	Finite volume / finite difference	Conservative radial flux	Finite volume
Time integration	Explicit / implicit / adaptive	Stability vs. cost	Fully implicit
Grid design	Uniform / logarithmic radial	Early-time resolution	Logarithmic
Nonlinearity solve	Newton / Picard	Convergence control	Newton with damping
Linear solver	Direct / Krylov + preconditioner	Sparse systems	GMRES + ILU
Time-step control	Fixed / error-based adaptivity	Captures fast transients	Adaptive

Table 7: Machine-learning-based inversion ingredients

Element	Role	Examples	Notes
Input vector $\mathbf{y}$	Observed transients	$p_w(t)$, $T(t)$, rates	Time-series structure
Target $\boldsymbol{\theta}$	Near-wellbore parameters	k, S, C_w	Low to moderate dimension
Model $f_{\boldsymbol{\omega}}$	Learn inverse map	CNN, RNN, transformers	Sequence-aware networks
Loss $\mathcal{L}$	Training objective	MSE + regularization	May be dimensionless
Uncertainty layer	Quantify posterior spread	Bayesian NN, ensembles	Supports risk-aware use
Training data	Supervision source	Synthetic simulations	Needs realistic noise

as

$$\frac{\partial p_D}{\partial t_D} = \frac{1}{r_D}\frac{\partial}{\partial r_D}\left([12] r_D \frac{\partial p_D}{\partial r_D}\right), \tag{12}$$

for the simplest case of constant properties and no sources outside the wellbore. Extensions to include composite regions, wellbore storage, and skin introduce additional dimensionless groups, but the rescaled equations highlight the similarity between systems that differ in absolute scale yet share the same dimensionless parameters. This similarity property is exploited extensively in both analytical interpretation and data-driven modeling of transient near-wellbore responses.

Analytical characterization of transient near-wellbore pressure and temperature behaviour

Analytical and semi-analytical solutions for near-wellbore flow provide valuable insight into the sensitivity of early-time transients to various physical mechanisms. For single-phase radial flow with constant properties in an infinite reservoir, the classical line-source solution describes the pressure response at radius r to a constant rate production or injection at the well [13]. In dimensionless form, the pressure at the wellbore under constant rate production can be expressed as an integral involving exponential and logarithmic terms. When wellbore storage is included, the observed sandface pressure becomes a convolution of the formation response with the storage behaviour, leading to characteristic early-time slopes in log-log plots of pressure and its derivative.

One convenient representation of wellbore storage effects is obtained in the Laplace domain. Let $\tilde{p}_D(s)$ denote the Laplace transform of the dimensionless wellbore pressure, with s the Laplace variable. For a unit rate drawdown test in a homogeneous reservoir with dimensionless wellbore storage C_D and skin factor S, the Laplace-space solution can be written in compact form as

$$\tilde{p}_D(s) = \frac{1}{s^2}\frac{1}{1 + C_D s\, f(s, S)}, \tag{13}$$

where $f(s, S)$ encapsulates the formation response, including the effect of skin. Inverse Laplace transformation yields the time-domain pressure, and the derivative of p_D with respect to $\ln t_D$ reveals distinct regimes such as the early wellbore storage regime, the intermediate radial flow regime, and the late-time boundary regime. Although closed-form expressions for $f(s, S)$ are not always available, approximations can be derived for specific time ranges, allowing asymptotic analysis of the derivative behaviour [14].

The presence of a composite near-wellbore zone modifies the early-time pressure response. For a two-region system with inner permeability k_s and outer permeability k_r, the effective skin factor at late times can be related to the log ratio of permeabilities and the thickness of the altered zone. However, the transient behaviour at intermediate times depends on the diffusivity contrast between regions and on the storage characteristics of each region. Analytical solutions for such systems can be constructed using Laplace transforms and continuity conditions at the interface $r = r_s$. In many cases, the wellbore pressure response is expressed as an integral involving Bessel functions and exponentials. For interpretive purposes, approximate expressions that capture the leading-order behaviour in short-time and intermediate-time limits are often sufficient.

Temperature transients provide complementary information about near-wellbore processes. In a simple model where a fluid of temperature T_{inj} is injected into a formation at initial temperature T_0, the temperature at the sandface evolves due to the competition between advective transport of the injected fluid, conductive heat exchange with the formation, and heat capacity of the combined

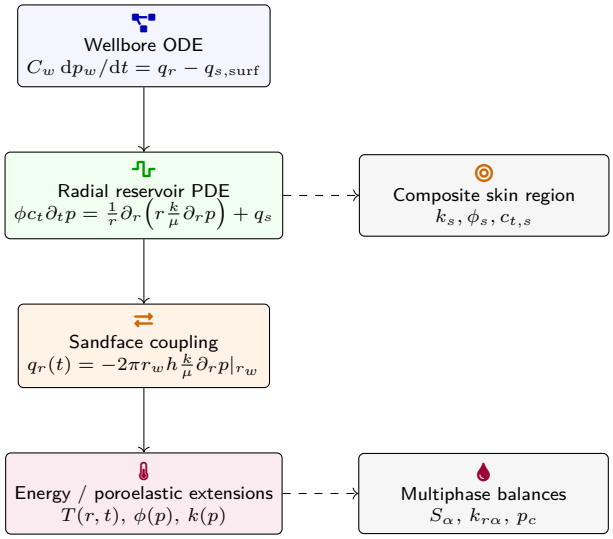

Figure 2: Structure of the governing equations linking the wellbore storage ordinary differential equation, the radial reservoir pressure diffusion equation, sandface coupling conditions, and optional thermal or poroelastic extensions, together with auxiliary composite-skin and multiphase formulations.

fluid-rock system. For constant injection rate and negligible variation of fluid properties with temperature, the energy equation in radial coordinates reduces to a form that can be linearized and solved using transforms analogous to those used for pressure [15]. The resulting solutions show that the early-time temperature change near the wellbore is dominated by the entering fluid, while at longer times conductive exchange and radial dispersion smooth the temperature profile.

Coupled pressure and temperature transients can reveal phenomena such as the Joule–Thomson effect and non-isothermal compressibility. When pressure changes occur rapidly near the wellbore, fluid temperature may change even in the absence of net heat exchange with the surroundings. In such cases, the energy equation includes source terms proportional to the time derivative of pressure, and analytical solutions must account for the coupling between the pressure diffusion equation and the energy balance. For small departures from an initial state, linearized models can be used in which temperature is expressed as a convolution of the pressure rate with a kernel determined by thermodynamic properties and formation characteristics. This convolution structure suggests that pressure and temperature measurements together can improve identifiability of near-wellbore properties compared to pressure alone [16].

Another important analytical avenue concerns non-Darcy flow and inertial effects in high-rate or gas-dominated wells. The Forchheimer correction introduces a quadratic term in the relationship between pressure gradient and velocity, leading to a modified flow law of the form

$$-\nabla p = \frac{\mu}{k}\mathbf{v} + \beta\rho|\mathbf{v}|\mathbf{v}, \tag{14}$$

with β an inertial coefficient. Substitution into the mass conservation equation produces a nonlinear partial differential equation in which the effective diffusivity depends on the magnitude of the velocity. Analytical solutions in closed form are generally not available, but perturbation methods can be applied when the non-Darcy term is small compared to the Darcy term [17]. Such analyses indicate that non-Darcy effects steepen early-time pressure gradients near the wellbore and can be interpreted, in certain regimes, as an apparent additional skin that depends on flow rate. Distinguishing this dynamic skin from true mechanical damage or stimulation requires careful consideration of rate dependence.

Dimensionless analysis plays a central role in classifying transient near-wellbore behaviour. By introducing dimensionless groups for time, radius, wellbore storage, and non-Darcy parameters, it is possible to construct regime maps that delineate domains in which different physical processes dominate. For example, the ratio of the characteristic diffusion time in the skin region to that in the far-field reservoir controls whether the altered zone appears as a distinct transient feature or only as a static skin in the observed signal [18]. Similarly, a dimensionless number involving the Forchheimer coefficient, rate, and permeability indicates the importance of inertial effects. Analytical approximations in each regime help to explain qualitative features observed in simulated or measured pressure derivatives, such as humps, inflection points, or changes in slope.

Temperature-based dimensionless groups involve ratios of conductive and advective time scales as well as the relative importance of Joule–Thomson heating or cooling. In cases where temperature is largely controlled by advective transport of injected fluid, the transient sandface temperature behaves approximately as a plug-flow signal with smoothing due to axial dispersion. When conductive exchange dominates, the temperature response reflects the

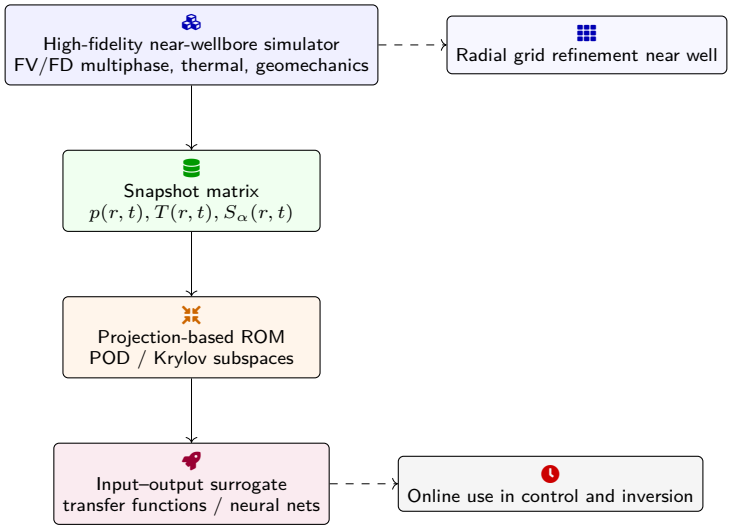

Figure 3: Workflow for numerical simulation and reduced-order modeling: detailed near-wellbore simulations on refined grids generate state snapshots, which feed projection-based reduced-order models; these are complemented by faster input–output surrogates that are suitable for online control and inversion tasks.

diffusion of a thermal front into the formation. Analytical solutions for these limiting cases can be used to calibrate semi-empirical models that interpolate between regimes, enabling approximate interpretation of temperature logs in terms of near-wellbore permeability and thermal properties [19].

The analytical characterization, while based on simplifying assumptions, establishes patterns and structures that guide both numerical simulation and data-driven interpretation. It identifies which combinations of parameters control key features of the response and how these features move or deform when properties change. This understanding is essential for constructing parameterizations for inversion, designing tests that maximize sensitivity to parameters of interest, and evaluating whether certain parameters are practically identifiable from available data. The analytical framework also informs the construction of synthetic data sets used to train and validate machine-learning models, by focusing attention on parameter ranges and regimes that are most relevant to near-wellbore phenomena in realistic wells.

Numerical simulation and reduced-order modeling of near-wellbore dynamics

Analytical solutions for near-wellbore flow and transport are limited in their ability to represent the full complexity of real wells, which may involve heterogeneous formations, complex completion geometries, multiphase flow, and nonlinear property variations with pressure and temperature. Numerical simulation provides a more general tool for resolving these complexities, at the cost of increased computational effort [20]. For transient near-wellbore phenomena, numerical schemes must capture steep gradients and short time scales near the well while maintaining stability and accuracy over longer periods and larger spatial domains.

Finite volume and finite difference methods are commonly used to discretize the radial diffusion equation and its generalizations. In a radial grid with cell centers at radii r_i and control volumes defined between midpoints, the discretized diffusion operator for a cell i may be expressed in conservative form as

$$\phi_i c_{t,i} \frac{p_i^{n+1} - p_i^n}{\Delta t} = \frac{1}{r_i} \left(F_{i+1/2}^{n+1} - F_{i-1/2}^{n+1} \right) + q_i^{n+1}, \quad (15)$$

where Δt is the time step, p_i^n is the pressure at time level n, and $F_{i+1/2}^{n+1}$ denotes the radial flux between cells i and $i+1$ evaluated at time $n+1$. For a homogeneous medium with constant k and μ, the flux can be approximated as

$$F_{i+1/2}^{n+1} = -r_{i+1/2} \frac{k}{\mu} \frac{p_{i+1}^{n+1} - p_i^{n+1}}{r_{i+1} - r_i}, \quad (16)$$

with $r_{i+1/2}$ a suitably defined interface radius. Implicit time discretization, as indicated by the use of $n+1$ in the fluxes, is generally preferred for stability, especially when time steps vary or when strong nonlinearities are present [21].

The coupling to the wellbore storage equation introduces an additional algebraic or differential equation at the innermost grid block. The radial flux from the reservoir into the well is computed from the discretized flux at the wellbore, and the wellbore pressure is either identified with the pressure in the first grid block or connected via an additional well index relation. The combined system at each time step can be written in matrix form as

$$\mathbf{A}\mathbf{p}^{n+1} = \mathbf{b}, \quad (17)$$

where $\mathbf{p}^{n+1}$ collects the pressures in all grid blocks and possibly the wellbore pressure. The matrix $\mathbf{A}$ is sparse, with a banded or near-banded structure in simple radial grids. For more complex geometries or coupled multiphase

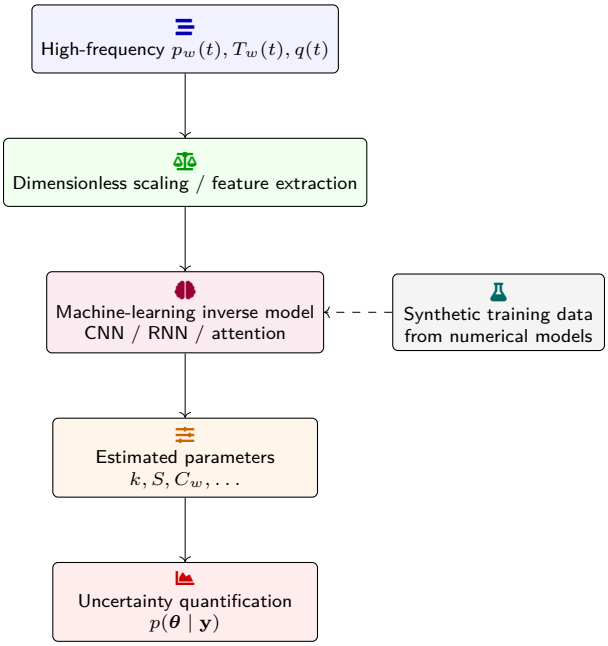

Figure 4: Machine-learning-based inversion of transient near-wellbore responses: high-frequency pressure, temperature, and rate signals are scaled and embedded, passed through a learned inverse model, and mapped to near-wellbore parameters together with probabilistic uncertainty estimates informed by synthetic training data.

systems, the structure can be more intricate, but it remains sparse.

Temporal discretization must resolve the characteristic diffusion time scales in the near-wellbore region [22]. A local diffusive time step criterion can be expressed as

$$\Delta t \leq \theta \frac{\phi_i c_{t,i} \Delta r_i^2}{k_i/\mu_i}, \tag{18}$$

with θ a parameter controlling accuracy. Fully implicit schemes relax strict stability limits but large time steps can still degrade accuracy in early-time transients. Adaptive time stepping that refines time steps during rapid changes in pressure or rate and coarsens them during slowly varying phases provides a compromise between resolution and computational efficiency [23]. Error estimators based on differences between first-order and higher-order time integration schemes, or on residual norms of the discretized equations, guide such adaptivity.

When multiphase flow, thermal effects, or poroelasticity are included, the governing equations form a coupled nonlinear system for pressures, saturations, temperatures, and possibly displacement fields. Newton-type methods are commonly used to solve these systems at each time step. Linearization yields Jacobian matrices that incorporate derivatives of fluxes and source terms with respect to primary variables. The resulting linear systems are typically solved using iterative Krylov subspace methods with preconditioning tailored to the block structure of the problem. In the near-wellbore context, strong coupling between pressure and saturation, or between pressure and temperature, can make convergence sensitive to time-step size and initial guesses, further motivating adaptive strategies [24].

Direct numerical simulation of the full near-wellbore dynamics for every candidate parameter set is computationally intensive and not always feasible for real-time interpretation or control. Reduced-order modeling offers a way to approximate the behaviour of the full system using a lower-dimensional representation constructed from a set of basis functions or snapshots. One common approach is projection-based model reduction, in which the state vector $\mathbf{p}(t)$ is approximated as

$$\mathbf{p}(t) \approx \mathbf{V}\mathbf{z}(t), \tag{19}$$

where $\mathbf{V}$ is a matrix whose columns are basis vectors and $\mathbf{z}(t)$ is a vector of reduced coordinates. The basis vectors may be obtained from proper orthogonal decomposition of simulated state trajectories or from Krylov subspace methods. Substitution into the full-order equations and projection onto the reduced space results in a system of reduced dimension for $\mathbf{z}(t)$ that can be integrated more efficiently.

Reduced-order models must retain sufficient fidelity in the near-wellbore region to accurately capture early-time transients. This requirement often motivates local enrichment of the basis near the well, or separate basis sets for near-wellbore and far-field regions [25]. Parameter dependence also poses challenges, as the basis constructed at one parameter set may not represent dynamics at another. Parameterized model reduction strategies, in which the basis adapts to changes in permeability, compressibility, or other parameters, are therefore of interest. Techniques such as interpolation of reduced-order models or global bases spanning a range of parameter values can be used, but they increase the offline

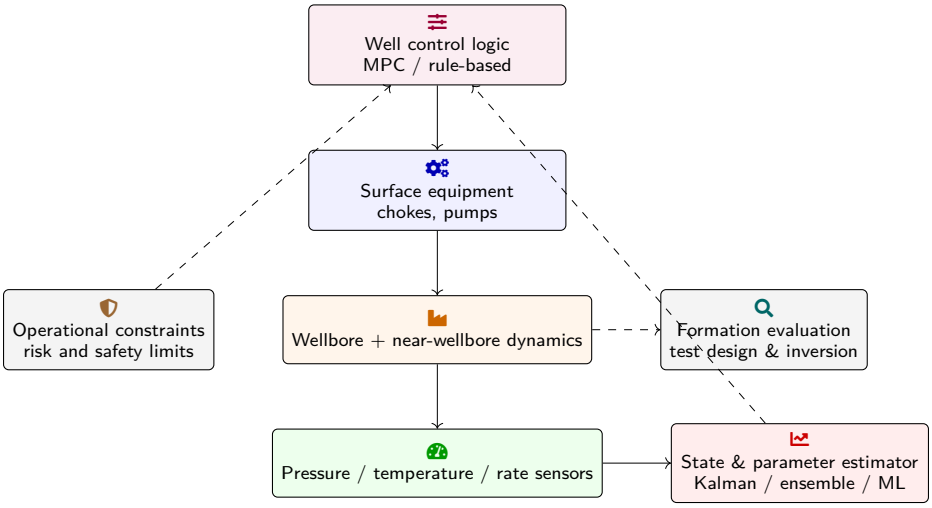

Figure 5: Integration of near-wellbore modeling into well control and formation evaluation: control actions at the surface propagate through the wellbore and near-wellbore region, measurements are fused in estimators that update states and parameters, and the resulting information feeds both operational decisions and interpretation workflows under explicit risk and constraint considerations.

computational effort required to construct the models.

Another class of reduced models is based on surrogate descriptions of the input-output behaviour of the system rather than its internal state. For near-wellbore phenomena, the inputs may include prescribed flow rates or choke settings, and the outputs are the measured pressures and temperatures at the wellbore. The mapping from inputs to outputs can be approximated by parametric transfer functions, autoregressive models with exogenous inputs, or nonlinear regressions [26]. For example, a discrete-time representation of the wellbore pressure response might have the form

$$p_w[n] = \sum_{k=1}^{N_a} a_k p_w[n-k] + \sum_{k=1}^{N_b} b_k q[n-k] + e[n], \quad (20)$$

where $q[n]$ is the rate at time index n, a_k and b_k are coefficients, and $e[n]$ is a residual term. The coefficients may depend on underlying formation properties, so the model can serve both as a predictive tool for simulation and as a component of an inversion algorithm.

Hybrid approaches that combine physics-based reduced-order models with data-driven components are well suited to near-wellbore applications. For instance, the structure of the diffusion equation dictates general features of the pressure response, such as smoothness and causality, while more complex or uncertain aspects, such as rate-dependent skin or nonlinear relative permeability curves, can be represented by data-driven corrections [27]. This division of labour allows the model to enforce physical constraints where they are clear and to learn flexible mappings where physics is less certain or too complex to model explicitly.

Numerical models are also crucial in generating synthetic data sets for training and testing machine-learning-based interpretation schemes. By sampling parameter spaces that include variability in permeability, skin, wellbore storage, relative permeability characteristics, and operational controls, one can produce ensembles of transient responses under various noise conditions. These synthetic data sets must be constructed carefully to avoid biases, to reflect plausible variability, and to ensure that the trained models generalize over the range of conditions expected in real wells. Grid resolution and time-step choices in the numerical simulations directly impact the quality of the synthetic data and therefore the performance of the learned models.

Machine-learning-based interpretation and probabilistic inversion of transient responses

Data-driven methods offer a complementary route to interpreting transient near-wellbore phenomena, particularly when the mapping from measured signals to formation properties is complex and not easily expressed in closed form [28]. Machine-learning models can approximate the inverse mapping from pressure and temperature time series, combined with operational inputs, to estimates of permeability, skin, wellbore storage, or more detailed near-wellbore descriptors. Such models are typically trained on synthetic data generated by numerical simulations, though they may also incorporate field data when available.

Consider a simplified setting in which the observable data vector $\mathbf{y}$ consists of sampled pressure and temperature values at the wellbore over a time window, while the parameter vector $\boldsymbol{\theta}$ includes quantities such as permeability k, skin factor S, storage coefficient C_w, and a small number of shape parameters describing heterogeneity in the near-wellbore region. The goal is to approximate a mapping

$$\hat{\boldsymbol{\theta}} = f_{\boldsymbol{\omega}}(\mathbf{y}), \quad (21)$$

where $f_{\boldsymbol{\omega}}$ is a parameterized function, for instance a neural network with weights and biases collected in $\boldsymbol{\omega}$. Training data consist of pairs $(\mathbf{y}^{(i)}, \boldsymbol{\theta}^{(i)})$ generated by sampling $\boldsymbol{\theta}^{(i)}$ from a prior distribution and computing the corresponding

transient response using the numerical model.

The training objective is often defined as a mean-squared error loss with regularization. For a batch of size N, the loss function can be written as

$$\mathcal{L}(\boldsymbol{\omega}) = \frac{1}{N}\sum_{i=1}^{N}\left\|[29]f_{\boldsymbol{\omega}}\left(\mathbf{y}^{(i)}\right) - \boldsymbol{\theta}^{(i)}\right\|_2^2 + \lambda\left\|\boldsymbol{\omega}\right\|_2^2, \quad (22)$$

with λ a regularization parameter. Optimization of $\mathcal{L}$ with respect to $\boldsymbol{\omega}$ is typically performed using stochastic gradient descent or its variants. The network architecture can exploit the temporal structure of the data by using one-dimensional convolutional layers, recurrent layers, or attention mechanisms designed for sequence data [30].

To enhance generalization and robustness, it is useful to work with dimensionless representations of both inputs and outputs. Pressures, temperatures, and times can be scaled using characteristic values derived from estimated ranges of parameters or from early-time measurements. For example, dimensionless time can be defined using an estimated diffusivity, and dimensionless pressure may be formed using a characteristic pressure drop. Such scaling reduces the variability in the data and can allow a single model to be applicable across wells and formations that share similar dimensionless descriptions, even if their absolute scales differ.

In addition to deterministic point estimates of $\boldsymbol{\theta}$, it is often important to quantify uncertainty. A probabilistic formulation seeks to characterize the posterior distribution $p(\boldsymbol{\theta} \mid \mathbf{y})$ given observed data. Bayesian approaches express this posterior as proportional to the product of a likelihood $p(\mathbf{y} \mid \boldsymbol{\theta})$ and a prior $p(\boldsymbol{\theta})$. When the numerical model is available, the likelihood can be approximated by assuming additive observation noise, for example [31]

$$p(\mathbf{y} \mid \boldsymbol{\theta}) \propto \exp\left(-\frac{1}{2\sigma^2}\left\|\mathbf{y} - \mathbf{g}(\boldsymbol{\theta})\right\|_2^2\right), \quad (23)$$

where $\mathbf{g}(\boldsymbol{\theta})$ denotes the model-predicted data and σ^2 is a noise variance. Sampling from the posterior using Markov chain Monte Carlo is usually too slow for real-time applications, but approximate methods such as variational inference or ensemble-based approaches can provide useful estimates of uncertainty.

Machine-learning techniques can also be integrated directly into the solution of the governing equations through physics-informed neural networks [32]. In such approaches, a neural network is used to approximate the spatiotemporal pressure field $p(r,t)$, and the loss function includes terms that penalize violations of the differential equations and boundary conditions. For example, a loss function may include a residual term of the form

$$\mathcal{R} = \left(\phi c_t \frac{\partial \hat{p}}{\partial t} - \frac{1}{r}\frac{\partial}{\partial r}\left(r\frac{k}{\mu}\frac{\partial \hat{p}}{\partial r}\right) - q_s\right)^2, \quad (24)$$

where $\hat{p}$ is the neural network approximation of p. Minimization of the integral of $\mathcal{R}$ over sampling points in space and time, along with terms enforcing boundary conditions and data fit, encourages the network to represent physically consistent solutions. In a near-wellbore context, physics-informed networks can be used to interpolate sparse downhole measurements, to fill in unmeasured regions of the domain, or to embed known physics into a learning-based inversion [33].

Probabilistic machine-learning models such as Gaussian processes or Bayesian neural networks provide another route to uncertainty quantification. For instance, a Gaussian process prior on the mapping from dimensionless time to dimensionless pressure can capture smoothness assumptions and yield predictive distributions at unobserved times. If the hyperparameters of the covariance function are themselves related to formation properties, fitting the Gaussian process to observed transient data can indirectly estimate those properties. However, the computational cost of Gaussian processes scales poorly with the number of time samples, so sparse approximations or structured kernels are often needed for long time series.

An important consideration in machine-learning-based interpretation is identifiability: not all parameters influence the transient response in a distinguishable manner, especially in the presence of noise and limited test duration. Sensitivity analysis, either based on numerical derivatives of the model outputs with respect to parameters or on variance-based methods, helps to identify which parameters can be reliably inferred [34]. Machine-learning models may be designed to focus on a subset of parameters that are most influential and to treat others as nuisance variables integrated over during training. This focus can improve robustness and avoid overfitting to noise.

Validation of data-driven models requires evaluation on synthetic and, when available, field data that are not used for training. Statistical measures such as root-mean-square error in parameter estimates, coverage probabilities of confidence or credible intervals, and calibration of predicted uncertainties provide quantitative assessment. Because synthetic training data inevitably reflect modeling assumptions, discrepancies between synthetic and field responses must be examined carefully [35]. Domain adaptation techniques, in which the model is fine-tuned using limited field data or adjusted to account for systematic shifts in the data distribution, can mitigate some of these discrepancies.

Overall, machine-learning-based interpretation and probabilistic inversion offer flexibility in handling complex near-wellbore phenomena and integrating diverse data types. Their performance depends critically on the quality and representativeness of training data, the incorporation of physical constraints, and rigorous assessment of uncertainty. These considerations are particularly important when such models are used to support real-time well control decisions, where misinterpretation of transient signals may have operational consequences.

Near-wellbore modeling for well control and operational decision-making

Well control relies on timely detection and mitigation of undesired events such as influx of formation fluids into the wellbore, loss of circulation, and unstable flow regimes that can threaten safety or reduce operational efficiency. Transient near-wellbore phenomena are central to these processes, as they dictate how quickly pressure changes propagate, how the wellbore fluid column responds to formation interactions, and how control actions at the surface influence downhole conditions [36]. Modeling these dynamics provides a basis for designing detection algorithms, predicting the outcomes of control actions, and assessing margins of safety.

One useful representation of near-wellbore dynamics for control purposes is a reduced-order state-space model. By linearizing the governing equations around an operating point, it is possible to express the evolution of deviations in pressure and rate as a system of linear differential equations. For example, small perturbations $\delta p_w(t)$ in wellbore pressure and $\delta q(t)$ in flow rate may satisfy

$$\frac{d}{dt}\delta p_w(t) = a_{11}\delta p_w(t) + a_{12}\delta q(t) + d_1(t), \tag{25}$$

$$\frac{d}{dt}\delta x(t) = \mathbf{A}_x\delta x(t)[37] + \mathbf{B}_x\delta q(t) + \mathbf{d}_x(t), \tag{26}$$

where $\delta x(t)$ encodes additional state variables representing near-wellbore storage and pressure distribution. The matrices a_{11}, a_{12}, $\mathbf{A}_x$, and $\mathbf{B}_x$ are obtained by linearizing the diffusion and wellbore equations, and the perturbation terms $d_1(t)$ and $\mathbf{d}_x(t)$ represent unmodelled disturbances. Discretization in time leads to a model suitable for use in model predictive control or state estimation schemes such as Kalman filters.

Choke settings, pump rates, and other controllable inputs determine boundary conditions for the near-wellbore model. In a simple formulation, the surface-controlled rate $q_{s,\,surf}(t)$ appears directly in the wellbore storage equation and indirectly influences the formation pressure. Control strategies may seek to regulate wellbore pressure within prescribed limits, to maintain a desired drawdown profile, or to respond to detected anomalies in measured signals. The performance of such strategies depends on the accuracy with which the model represents near-wellbore dynamics and on the robustness of the control design to model uncertainties [38].

Detection of influxes or losses often relies on comparing measured pressure and rate signals with model predictions under normal conditions. Deviations that cannot be explained by expected operational changes may indicate that formation fluids are entering or leaving the wellbore in an unplanned manner. A near-wellbore model that accounts for storage, skin, and temperature-dependent properties can reduce false alarms by providing a more accurate baseline response. For instance, a step change in choke opening produces a characteristic transient pressure response at the sandface, whose shape depends on near-wellbore parameters. If the observed response deviates significantly from the modeled baseline in a manner consistent with additional inflow or outflow, this may trigger an alarm [39].

Statistical change detection methods can be built on residuals between measured and predicted signals. Let $\hat{p}_w(t)$ be the model-predicted pressure and $p_w^{\text{meas}}(t)$ the measured pressure. The residual $r(t) = p_w^{\text{meas}}(t) - \hat{p}_w(t)$ can be monitored using thresholds or more sophisticated statistics that account for noise and model uncertainty. Sequential probability ratio tests or cumulative sum techniques can be adapted to operate on these residuals. The choice of thresholds involves a trade-off between false positive and false negative rates, and near-wellbore models help by reducing systematic biases and making residuals more stationary under normal conditions.

Machine-learning models trained on transient responses can also support well control by providing fast evaluations of expected pressure or temperature under different control actions. For example, a surrogate model may predict the sandface pressure response to a proposed change in choke opening or pump rate, allowing operators to assess whether pressure limits are likely to be violated. Such surrogates can be embedded in optimization routines that search over control actions to achieve multiple objectives, such as maximizing rate while maintaining pressure within bounds and limiting the risk of reaching critical gradients near the wellbore [40].

Uncertainty in formation properties and near-wellbore conditions affects the reliability of control decisions. Probabilistic models of near-wellbore dynamics allow computation of distributions over future pressures and flows under candidate control strategies. These distributions can be used to evaluate probabilities of exceeding safety limits or triggering undesired events. Control policies that manage risk, such as those based on chance constraints or robust optimization, can be formulated in this probabilistic setting. The integration of transient near-wellbore modeling, probabilistic inversion of formation properties, and risk-aware control thus forms a coherent framework, even though each component carries its own approximations.

Operational constraints, such as limits on the rate of change of choke positions or delays in measuring downhole pressures, must be incorporated into the control design [41]. Delays are particularly relevant when only surface measurements are available and must be interpreted through the model to infer downhole conditions. The near-wellbore model provides a mapping from surface pressures and rates to sandface pressures and flows, but this mapping is subject to uncertainty and latency. State estimation methods, including extended or ensemble Kalman filters, can combine model predictions with available measurements to estimate the hidden states and parameters in real time, thereby improving the basis for control actions.

In addition to safety considerations, near-wellbore modeling can inform operational choices that influence formation evaluation. For example, the design of drawdown and buildup sequences during testing can be optimized to maximize sensitivity to parameters of interest while respecting well control constraints. By simulating candidate test sequences with the near-wellbore model and evaluating the resulting Fisher information matrix or related measures of parameter sensitivity, one can identify test designs that are more informative [42]. This coupling between control and evaluation illustrates how near-wellbore modeling serves both operational and interpretive roles.

Formation evaluation and parameter estimation from transient near-wellbore data

Formation evaluation traditionally combines petrophysical logs, core measurements, and well test analysis to infer permeability, porosity, fluid properties, and other reservoir characteristics. Transient near-wellbore data, including short-time pressure and temperature responses to controlled flow rate changes, provide additional information that can refine these estimates, particularly in the vicinity of the well. A central challenge is to formulate parameter estimation procedures that account for the complex, coupled nature of the near-wellbore system while remaining computationally feasible and robust to uncertainties.

Inverse problems for near-wellbore parameter estimation are commonly posed as optimization problems in which the objective is to minimize the misfit between observed and modeled data. Let $\mathbf{d}^{\text{obs}}$ represent a vector of observed pressures and temperatures at discrete times, and let $\mathbf{d}(\boldsymbol{\theta})$ denote the corresponding predictions of the near-wellbore model for a parameter vector $\boldsymbol{\theta}$. A least-squares objective function takes the form

$$J(\boldsymbol{\theta}) = \frac{1}{2} \left(\mathbf{d}(\boldsymbol{\theta}) - \mathbf{d}^{\text{obs}} \right)^{\mathsf{T}} \mathbf{W} \left(\mathbf{d}(\boldsymbol{\theta}) - \mathbf{d}^{\text{obs}} \right), \tag{27}$$

where $\mathbf{W}$ is a weighting matrix, often chosen as the inverse of the noise covariance matrix when known. Minimizing $J(\boldsymbol{\theta})$ with respect to $\boldsymbol{\theta}$ yields parameter estimates that best fit the data in the weighted least-squares sense, subject to the validity of the model and noise assumptions.

Gradient-based methods are efficient for solving such optimization problems when the dimension of $\boldsymbol{\theta}$ is moderate and derivatives of $\mathbf{d}(\boldsymbol{\theta})$ with respect to parameters can be computed accurately. Adjoint techniques are particularly useful in this context. By deriving and solving the adjoint equations associated with the near-wellbore model, one can evaluate the gradient $\nabla_{\boldsymbol{\theta}} J$ at a cost comparable to that of one or a few forward simulations, independent of the number of parameters. This efficiency enables the use of second-order or quasi-Newton methods that can converge rapidly to local minima [43].

The ill-posed nature of inverse problems necessitates regularization. Prior information about parameters, such as expected ranges of permeability or skin factors, can be encoded through penalty terms added to the objective function. For instance, a quadratic regularization term

$$J_{\text{reg}}(\boldsymbol{\theta}) = \frac{\gamma}{2} \left\| \boldsymbol{\theta} - \boldsymbol{\theta}_0 \right\|_2^2 \tag{28}$$

penalizes deviations from a prior mean $\boldsymbol{\theta}_0$ with strength controlled by γ. More complex regularization, such as sparsity-promoting norms or structural constraints reflecting expected relationships between parameters, can also be employed. These choices influence the stability of the inversion and the balance between fitting the data and adhering to prior knowledge [44].

Statistical assessment of parameter estimates can be based on linearized approximations of the inverse problem. Near an estimated parameter vector $\hat{\boldsymbol{\theta}}$, the covariance of the estimation error may be approximated by the inverse of the Fisher information matrix

$$\mathbf{I} = \mathbf{G}^{\mathsf{T}} \mathbf{W} \mathbf{G}, \tag{29}$$

where $\mathbf{G}$ is the sensitivity matrix with elements $G_{ij} = \partial d_i / \partial \theta_j$ evaluated at $\hat{\boldsymbol{\theta}}$. The eigenvalues and eigenvectors of $\mathbf{I}$ reveal directions in parameter space that are well or poorly constrained by the data. Parameters associated with small eigenvalues of $\mathbf{I}$ are difficult to estimate reliably, and attempts to infer them may lead to overfitting and unstable solutions. This analysis can inform the choice of parameterization, suggesting simplifications or aggregations when necessary.

Incorporating near-wellbore transients into formation evaluation requires integration with other data sources. For example, core and log measurements provide local estimates of porosity and permeability, which can be used as priors in the inversion. Seismic data may inform larger-scale heterogeneity patterns that affect the far-field pressure response. Joint inversion frameworks that combine near-wellbore transients with other measurements can, in principle, provide more coherent estimates, but they also increase model complexity and computational cost [45]. Careful selection of which parameters to treat as global (shared across data sets) and which to treat as local (specific to the near-wellbore region) is important for tractable formulations.

Short-time transients are particularly sensitive to very near-wellbore properties, such as the permeability and thickness of damaged or stimulated zones. However, these properties may vary around the circumference of the well and along its length, leading to anisotropic and three-dimensional effects. Representing such variability in an axisymmetric model requires effective parameters that average over azimuthal variations. In some cases, deviations from axisymmetry manifest as irregularities or azimuthally dependent signatures in distributed measurements, but these are difficult to resolve with limited data [46]. Parameterizations that capture the principal effects of heterogeneity with a small number of effective parameters are therefore often preferred, even though they cannot represent all details.

The role of temperature data in formation evaluation continues to expand with the increased availability of distributed temperature sensing. Transient temperature profiles along the well can reveal flow contributions from different zones, phase changes, and near-wellbore thermal properties. Inverse methods that jointly consider pressure and temperature data face additional challenges because the energy equation introduces further parameters, such as effective thermal conductivities and heat capacities. Nevertheless, joint inversion can reduce ambiguity for some parameters, as pressure and temperature respond differently to changes in properties. The design of observation strategies that exploit this complementarity is an active area of development.

Under operational constraints, data acquisition for formation evaluation must coexist with production or injection activities. Specialized tests, such as pressure pulses or step-rate tests, are designed to produce transient responses that are informative about specific parameters while staying within safe operating envelopes. Near-wellbore modeling supports the design of such tests by predicting their impact on wellbore and formation conditions and by quantifying expected sensitivities. The interplay between test design, parameter identifiability, and operational risk underscores the need for integrated approaches to formation evaluation that use transient near-wellbore phenomena as one of several complementary sources of information.

Conclusion

Transient near-wellbore phenomena arise from the interplay of fluid flow, energy transport, and mechanical effects in the immediate vicinity of a well. They are encoded in pressure, temperature, and flow-rate signals measured at the wellbore and offer opportunities for improved well control and formation evaluation, while also introducing complexities in interpretation [47]. This work has outlined a mathematical and computational framework for modeling these phenomena, explored analytical and numerical approaches to characterizing their behaviour, and discussed data-driven and statistical techniques for interpreting the resulting transients.

Starting from conservation laws in cylindrical coordinates, the analysis considered single-phase and multiphase flow, thermal coupling, and poroelastic effects, highlighting how each modifies the near-wellbore pressure and temperature responses. Analytical solutions and asymptotic analyses help identify dimensionless groups and regimes in which particular mechanisms dominate. Numerical discretization schemes, combined with wellbore storage models, enable simulation of more complex configurations that include heterogeneity, nonlinear property variations, and operational controls. Reduced-order models and surrogates provide computationally efficient approximations suitable for use in interpretation and control.

Machine-learning-based methods extend the interpretive toolkit by approximating inverse mappings from transient data to near-wellbore parameters and by quantifying uncertainties [48]. The success of these methods depends on careful construction of synthetic training data, integration of physical constraints into learning architectures, and rigorous validation against independent data. Probabilistic formulations and sensitivity analyses clarify which parameters can be reliably inferred and which remain weakly constrained, informing both parameterization choices and expectations about the level of detail attainable from transient data.

In well control applications, near-wellbore models support the design of detection algorithms, control strategies, and test protocols that respect safety constraints while making use of available information in transient signals. For formation evaluation, they offer a means to refine estimates of local properties, particularly in damaged or stimulated zones, and to integrate pressure and temperature data with other measurements. The overall picture is one in which transient near-wellbore phenomena are neither neglected nor overemphasized, but treated as a component of a broader modeling and interpretation framework that explicitly accounts for uncertainties and limitations. Continued development of models, numerical methods, and data-driven techniques, together with increased availability of high-resolution measurements, is expected to gradually improve the practical use of near-wellbore transients in both operational and evaluative contexts [49].

Conflict of interest

Authors state no conflict of interest.

References

[1] J. Nielsen, *The desorption kinetics of methane from nonaqueous fluids for enhanced well control*, Dec. 10, 2019. DOI: 10.31390/gradschool_theses.5054

[2] *Oil shale, tar sand, coal research, advanced exploratory process technology, jointly sponsored research. quarterly technical progress report, july–september 1992*, Dec. 31, 1992. DOI: 10.2172/10124838

[3] N. Jeyaprakash, C.-H. Yang, and M. B. Kumar, "Laser machining," in IntechOpen, Jul. 14, 2021. DOI: 10.5772/intechopen.93779

[4] C. Obi, Y. Falola, K. Manikonda, A. Hasan, I. Hassan, and M. Rahman, "A machine learning approach for gas kick identification," *SPE Drilling & Completion*, vol. 38, no. 04, pp. 663–681, 2023.

[5] *Permit to operate injection well ks-3*, Sep. 4, 1991. DOI: 10.2172/882360

[6] *Vocs in non-arid soils integrated demonstration: Technology summary*, Feb. 1, 1994. DOI: 10.2172/10135812

[7] I. T. Llc, *Advanced ultra-high speed motor for drilling*, Mar. 31, 2007. DOI: 10.2172/917759

[8] C. E. Tyner, *Minimum bed parameters for in situ processing of oil shale. first quarterly report, october 1-december 31, 1979*, Jan. 1, 1980. DOI: 10.2172/5655688

[9] J. Chimahusky, L. Hallenbeck, K. Harpole, and K. Dollens, *Design and implementation of a cosub 2 flood utilizing advanced reservoir characterization and horizontal injection wells in a shallow shelf carbonate approaching waterflood depletion. annual report, july 1, 1995–june 30, 1996*, May 1, 1997. DOI: 10.2172/513534

[10] M. H. Mahmoud, "Underwater precast reinforced concrete silo for oil drilling and production applications," in *Offshore Technology Conference*, OTC, May 1, 2017. DOI: 10.4043/27660-ms

[11] A. V. Muravyev, "Gas condensate wells: Challenges of sampling, testing and production optimization," *Energies*, vol. 15, no. 15, pp. 5419–5419, Jul. 27, 2022. DOI: 10.3390/en15155419

[12] K. Y, "Statistical and numerical investigation of the effect of wellbore trajectories in williston basin horizontal wells and their effects on production performance," *Petroleum & Petrochemical Engineering Journal*, vol. 6, no. 4, pp. 1–15, Oct. 20, 2022. DOI: 10.23880/ppej-16000320

[13] H. Liu and Q. Cheng, "An analysis of design and equipment of field waste-free system in drilling," *International Journal of Science and Research (IJSR)*, vol. 5, no. 6, pp. 281–285, Jun. 5, 2016. DOI: 10.21275/v5i6.nov164174

[14] F. H. Milburn and R. H. Williams, "Hoover/diana: Topsides," in *Offshore Technology Conference*, OTC, Apr. 30, 2001. DOI: 10.4043/13083-ms

[15] A. S. A. Sheidi et al., "Step change in controlling the gas-cap in highly depleted and fractured formation," in *ADIPEC*, SPE, Oct. 31, 2022. DOI: 10.2118/211490-ms

[16] L. Nokleberg, R. B. Schulle, and T. Sontvedt, "Shallow gas kicks, safety aspects related to diverter system," *SPE Offshore Europe*, Sep. 8, 1987. DOI: 10.2118/16545-ms

[17] J. H. Woo, J.-H. Nam, and K. H. Ko, "Development of a simulation method for the subsea production system," *Journal of Computational Design and Engineering*, vol. 1, no. 3, pp. 173–186, Jul. 1, 2014. DOI: 10.7315/jcde.2014.017

[18] *Energy technologies at sandia national laboratories: Past, present, future*, Aug. 1, 1989. DOI: 10.2172/5495888

[19] *Department of petroleum engineering and center for petroleum and geosystems engineering annual report, 1990–1991 academic year*, Dec. 31, 1991. DOI: 10.2172/10184021

[20] A. Malagalage and B. Halvorsen, "Near well simulation and modelling of oil production from heavy oil reservoirs," in *Linköping Electronic Conference Proceedings*, vol. 119, Linköping University Electronic Press, Nov. 25, 2015, pp. 289–298. DOI: 10.3384/ecp15119289

[21] Q. Nie, S. Zhang, Y. Huang, X. Yi, and J. Wu, "Numerical and experimental investigation on safety of downhole solid–liquid separator for natural gas hydrate exploitation," *Energies*, vol. 15, no. 15, pp. 5649–5649, Aug. 4, 2022. DOI: 10.3390/en15155649

[22] *Contracts for field projects and supporting research on enhanced oil recovery. progress review number 87*, Oct. 1, 1997. DOI: 10.2172/564048

[23] F. Loux et al., "Managed pressure drilling significantly reduces drilling costs on extremely challenging ultraht wells in the gulf of thailand," in *SPE/IATMI Asia Pacific Oil & Gas Conference and Exhibition*, SPE, Oct. 20, 2015. DOI: 10.2118/176046-ms

[24] H. Shrivastava, *Design/operations review of core sampling trucks and associated equipment*, Mar. 11, 1996. DOI: 10.2172/483423

[25] V. O. Yablonskii, "Modeling of degassing of viscoplastic liquids in a cylindrical hydrocyclone," *Russian Journal of Applied Chemistry*, vol. 95, no. 2, pp. 270–276, Jun. 15, 2022. DOI: 10.1134/s1070427222020069

[26] A. R. Hasan, K. Manikonda, M. Jang, M. A. Rahman, and G. Hashmi, "Estimating near-wellbore cooling due to drilling circulation and its effect on drill stem test," in *SPE Annual Technical Conference and Exhibition?*, SPE, 2024, D021S015R003.

[27] C.-H. Yang, P.-P. Lu, Y.-M. Cao, M. Xu, Z.-Y. Yu, and P.-F. Cheng, "Study on the plugging limit and combination of co2 displacement flow control system based on nuclear magnetic resonance (nmr)," *Processes*, vol. 10, no. 7, pp. 1342–1342, Jul. 10, 2022. DOI: 10.3390/pr10071342

[28] L. Kozlov et al., "Algorithm of controlling an adaptive hydraulic circuit for mobile machines," *International Journal of Modern Manufacturing Technologies*, vol. 13, no. 3, pp. 79–86, Dec. 25, 2021. DOI: 10.54684/ijmmt.2021.13.3.79

[29] *Western energy resources and the environment: Geothermal energy*, May 1, 1977. DOI: 10.2172/860618

[30] *Contracts for field projects and supporting research on enhanced oil recovery. progress review no. 80. quarterly report, july–september, 1994*, Nov. 1, 1995. DOI: 10.2172/172132

[31] *Deep drilling basic research: Volume 5 - system evaluations. final report, november 1988–august 1990*, Jun. 1, 1990. DOI: 10.2172/882934

[32] *Low-to-moderate-temperature hydrothermal reservoir engineering handbook. [appendices]*, Jun. 1, 1982. DOI: 10.2172/5281779

[33] *Feasibility study of a hybrid erosion drilling concept*, Jun. 1, 1977. DOI: 10.2172/5781385

[34] S. A. Cox, R. P. Stoltz, R. P. Sutton, R. D. Barree, and M. Conway, "Evaluation of the effect of complex reservoir geometries and completion practices on production analysis," in *Eastern Regional Meeting*, SPE, Oct. 17, 2007. DOI: 10.2118/111285-ms

[35] D. Ojedeji, *Gas evolution phenomenon of methane in base fluids of non-aqueous drilling muds under controlled depressurization*, Jun. 4, 2021. DOI: 10.31390/gradschool_theses.5420

[36] V. Simlote and C. Hearn, "Paddle river gas field, alberta, canada - evaluation of gas reserves and future operating strategy," in *SPE Annual Fall Technical Conference and Exhibition*, SPE, Oct. 1, 1978. DOI: 10.2118/7466-ms

[37] L. Lou, M.-j. Chen, W.-y. Qin, W.-r. Wu, and H.-y. Rui, "Research on the synchronization and shock characteristics of an air adjustment mechanism for cluster-type dth hammers under partial loads," *Shock and Vibration*, vol. 2022, pp. 1–17, Mar. 31, 2022. DOI: 10.1155/2022/9794391

[38] S. C. Soni, A. Bhargava, A. B. Desai, R. Kumar, and H. G. Suryadi, "Continuous improvement in drilling with rotary steerable system in mumbai high field.," in *SPE Oil and Gas India Conference and Exhibition*, SPE, Mar. 28, 2012. DOI: 10.2118/154823-ms

[39] A. T. Bozdana, N. -Al-Kharkhi, and K. Al-Kharkhi, "Comparative experimental and numerical investigation on electrical discharge drilling of aisi 304 using circular and elliptical electrodes," *Strojniški vestnik - Journal of Mechanical Engineering*, Apr. 15, 2018. DOI: 10.5545/sv-jme.2017.4806

[40] O. Baris, L. F. Ayala, and W. W. Robert, "Numerical modeling of foam drilling hydraulics," *The Journal of Engineering Research [TJER]*, vol. 4, no. 1, pp. 103–119, Dec. 1, 2007. DOI: 10.24200/tjer.vol4iss1pp103-119

[41] G. Muktadir, M. Amro, and A. Schramm, "Review and applicability of downhole separation technology," in *SPE Middle East Artificial Lift Conference and Exhibition*, SPE, Nov. 30, 2016. DOI: 10.2118/184201-ms

[42] M. Okot, M. Campos, G. Muñoz, A. Alalsayednassir, M. Weber, and Z. Muneer, "Utilization of an innovative tool to improve hole cleaning efficiency in extended reach wells in saudi arabia," in *SPE Kuwait Oil and Gas Show and Conference*, SPE, Oct. 11, 2015. DOI: 10.2118/175165-ms

[43] B. Harder, *Analysis of environmental constraints on expanding reserves in current and future reservoirs in wetlands. final report*, Mar. 1, 1995. DOI: 10.2172/43775

[44] R. Wemple, *Safety and emergency preparedness considerations for geotechnical field operations*, Apr. 1, 1989. DOI: 10.2172/6309062

[45] J. Tester, D. Brown, and R. Potter, *Hot dry rock geothermal energy— a new energy agenda for the twenty-first century*, Jul. 1, 1989. DOI: 10.2172/5620783

[46] L. Payne, "The effect of circulating media and nozzle design on rock bit performance," *Journal of Petroleum Technology*, vol. 4, no. 01, pp. 9–13, Jan. 1, 1952. DOI: 10.2118/144-g

[47] *Western gas sands project: Status report*, May 1, 1978. DOI: 10.2172/6743576

[48] B. Wang, L. Wang, X. Liu, and F. Ren, "Bifurcation diagram and dynamic response of a drill string applied in ngh drilling," *Processes*, vol. 10, no. 6, pp. 1111–1111, Jun. 2, 2022. DOI: 10.3390/pr10061111

[49] T. McVey, *Final report: Technoeconomic evaluation of undergroundcoal gasification (ucg) for power generationand synthetic natural gas*, Jun. 15, 2011. DOI: 10.2172/1118020